Waste to Energy System Based on Solid Oxide Fuel Cells: Department Store Case

Marvin M. Rokni
Technical University of Denmark, Dept. Mechanical Engineering, Section for Thermal Energy, Copenhagen, 2800, Denmark
E-mail:MR@mek.dtu.dk

Abstract

This study presents a new sustainable poly-generation system (power, heat, cool and freshwater) based on a solid oxide fuel cell (SOFC) system integrated with an absorption chiller and freshwater desalination system. The idea is to gasify the municipal waste of department stores in Denmark and thereby producing syngas, which serves as fuel for the poly-generation system. The proposed system recovers the waste heat to generate cooling and freshwater. Such advanced waste to energy systems when improved is self-sustainable, less disposal to sanitary landfills, saving large municipal fields for other human activity and considerable less environmental impact. The study shows that for a plant with about 145 kW net power, the energy efficiency may be more than 92% including electricity, cooling and freshwater production. For the case studied here, the cooling and freshwater productions will be about 145 kW and 180 liter/hour, respectively when the waste heat is equally divided between absorption chiller and freshwater desalination.

Keywords: Waste to energy; SOFC; municipal waste; renewable energy; poly-generation.

1. Introduction

Micro systems for combined cool, power and freshwater production falls into the category of small-scale multi-generation distributed systems at a single location that allows production and distribution. However, micro systems face the problem of secondary production in relation to power (such as cool/heat-to-power and/or freshwater-to-power) that varies daily and seasonally due to the different consumption profile [1]. Therefore, smart system designs are essential to address this problem.

The increase in municipal wastes (MW) of department stores has been significantly during the past decades due to increasing populations and income. Such significant increase is already a huge problem for many cities around the world. Waste to energy systems present some advantages such as reduction of greenhouse gas emissions and possibility of reducing landfills for storage of waste. Further, efficient waste management strategy is becoming a matter of crucial importance for our societies because of losing a huge amount of raw materials. Establishing efficient and innovative public policies to handle and exploit MW seems to be necessarily. Traditionally waste disposal in sanitary landfills is the widespread method related to waste management. Today this method is outdated due to two main facts; negative environmental impact and high demand of large fields reserved for waste disposal. Waste–to–energy systems may solve many of such problems [2]. Currently, the most established technology is incineration, while gasification is still in the early stages of development. The remaining waste after established separation and recycling technologies (such as plastics, metals, papers, glass bottles and hard papers) offers the basis to consider waste gasification as an alternative technology, which is also idea the main idea of the current study.

The definition of gasification is the thermal conversion of organic material into combustible gas. The transformation is performed by heating the feedstock with the presence of a gasification agent and by controlling the agent flow rate in the gasification process it is possible to perform an incomplete combustion of the feedstock and convert solid heterogeneous material to a gaseous fuel usable, see e.g. [3]. On average, conventional waste-to-energy plants that use mass-burn incineration can convert one ton of MW to about 550 kilowatt-hours of electricity. With gasification technology, one ton of MW can produce up to 1000 kilowatt-hours of electricity, meaning that MW gasification

is a much more efficient and cleaner way to utilize compared to waste incineration, see e.g. [4]. Despite its many advantages, biomass and waste gasification have yet represent about 0.33% of the global gasification capacity worldwide, but has potential to increase as discussed in [5]. Gasification is becoming an increasingly attractive alternative to incineration due to its pollution minimization effects, higher overall efficiency and ability to produce a clean and portable gas such as gasification of Portuguese waste [6]. However, due to environmental regulations post cleaning systems of waste incineration shows lower attraction compared to waste gasification and syngas cleaning systems, see e.g. [7]. Waste generation and composition is related to socio-economic factors as discussed in e.g. [8] and therefore shall be limited to a region or country. There are some examples of waste gasification for example waste food gasification [9] and municipal solid waste gasification [10].

Many studies explored SOFC (solid oxide fuel cell) based hybrid systems with high thermal efficiency. The majority of these studies use the waste heat from the SOFC system to run gas turbines resulting in expensive pressurized SOFC systems (with related technological problem) see e.g. [11]. Some studies such as [12] suggest to use the waste heat form the SOFC plants to derive steam turbines or organic Rankine cycles (ORC) resulting in non-pressurized SOFC stacks. A few studies utilizes the waste heat from the SOFC systems to route a heat engine as the bottoming cycle, see e.g. [13]. Studies on combined SOFC-absorption chillers (AC) are very limited. For example, Ref. [14] addressed a simple SOFC–AC system while Ref. [15] looked into the economic aspects of a SOFC–AC integrated. However, no studies have been found to drive a freshwater desalination system using waste heat from the SOFC plant, which is also forming the basis idea of the current study.

This study presents an inventive and smart waste to energy system that utilizes waste gasification technology to produce electricity, cooling and freshwater, through a SOFC plant, a double stage AC unit and a freshwater distillation device, respectively. No other studies reflect such ploy-generation system based on waste gasification plant, SOFC system, freshwater distillation device and an absorption chiller unit. Each model is validated against available experimental data. The current study is shall be viewed as author strive on designing sustainable future waste-to-energy poly-generation systems. All plant designs as well as all finding are new and have not been investigated elsewhere.

2. Methodology and Efficiency

The obtained thermodynamic results in this study are from the Dynamic Network Analysis (DNA) simulation tool (see, e.g. [16]. This software is a result of an ongoing development process in the section for Thermal Energy at the Technical University of Denmark (DTU). This software includes models for the thermodynamic state of many different fluids as well as standard numerical solvers for differential (and algebraic) equation systems. The component library models include heat exchangers, compressors, pumps, fuels cells, burners, absorbers, generators, condensers, evaporators, mixtures, desalinations, among many others. The thermodynamic state models for fluids cover most of the basic fluids as well as compounds such as ash and tar for use in energy system analyses.

This study expresses the energy efficiency as the ratio between the summations of net electric power with freshwater and district cooling, to the power of the fuel. The net electric power refers to the difference between the total produced power and the power consumed in the auxiliary components such as compressors, pumps, blowers, etc. The following equations express the plant efficiency (called also as energy efficiency or fuel utilization) and the electric efficiency defined in this study

$$\eta_{plant} = \frac{P_{Net}+Q_{FW}+P_{DC}}{\dot{m}_{fuel}LHV_{fuel}} \quad (1)$$

$$\eta_{el} = \frac{P_{Net}}{\dot{m}_{fuel}LHV_{fuel}} \quad (2)$$

where Q_{FW} and P_{DC} are the freshwater and district cooling (or domestic cooling) respectively. P_{Net} is the net power of the plant, LHV_{fuel} is the lower heating value of the fuel and $\dot{m}_{fuel}$ is the mass flow of the fuel.

2.1 Municipal Waste of Department Stores in Denmark

One should view the municipal waste as a feedstock, a fuel, and/or a potentially useful material. In this new light, the analyst must then seek to determine values for the physical and chemical engineering properties that, although less consistent than those of conventional materials and fossil fuels, nonetheless are the defining measures that characterize behavior. It is also necessarily that one must discard the sense that such wastes are so heterogeneous in theirs composition and very variable in theirs properties that will often exhibit great variability point-to-point and over time. Therefore, the designer must provide processes with more operating flexibility and reserve capacity than conventional process equipment. Further, waste management and optimization of resource recovery require reliable data on solid waste generation and composition.

Combustion processes (incineration) oxidize the organic fraction of waste fully and at high temperatures to form carbon dioxide and water vapor, plus quantities of acid gases, organic compounds, and particulate matter that contains some heavy metals. Combustion processes generate hot flue gas from which one can recover heat to generate steam and ultimately electricity through a Rankine cycle. However, due to environmental regulations, very sophisticated post-cleaning systems for the hot gases are essential requirements. Unlike the inherent simplicity of mass burn systems, gasification process convert the MW into useable gases called for syngas, usable for variety purposes. Such conversion technology requires that the flow sheet include a number of steps, including waste preprocessing, heating, and ultimately gasification, followed by somewhat sophisticated gas cleanup system. The heat released during gasification together with moisture content varies greatly between different material fractions and therefore the designer should check the system against different waste compositions.

2.2 Modeling of Gasifier

The present study uses the gasification model developed in a [12]. For clarity, this paper presents briefly the model. A simple Gibbs reactor, upon reaching chemical equilibrium, calculates the gas composition at a specified temperature and pressure without considering the reaction pathways by minimizing the total Gibbs free energy [17]. In such modeling, one achieves flow conservation of each constituent by taking into account that each element in the inlet gas is in balance with the outlet gas composition. Molar fraction of each element expresses such balance between inlet and outlet. The minimization of the Gibbs free energy is mathematically formulated by introducing a Lagrange multiplier (μ) for each chemical compound/constraints. By setting the partial derivative of the equation for each element to zero with respect to molar outlet flow, one can minimize the corresponding function. The model also includes a parameter for calibration of the compounds by bypassing some of the methane through the gasifier model. The reason is that the methane reaction is so fast that the model may underestimate the methane content at the outlet compare to a real gasifier. Here, the calibration id made by comparing the outlet gases with syngas from a real biomass gasifier as explained in Ref. [12]. With other words, the present study assumes that one percent of the methane bypasses the gasifier. Comparison between the model and the actual biomass gasifier developed at DTU resulted in this value.

Figure 1 displays the gasification plant modelled in this study. MW is fed continuously to a dryer, where most of the moisture is removed via a steam loop. This steam loop ensures that the moisture extracted from the waste feeds to the gasifier as gasification agent. Note that in reality, the dryer works also as pyrolysis. The dried waste feeds the gasifier while the moisture removed from the waste will mix with the preheated air before entering the gasifier. Thus, the gasification agent is the mixture of steam and air. A small pump in the colder side of the steam loop drives the loop and make sure continuous supply of the steam to the gasifier. Air preheats in a heat exchanger (GAP in the figure) and then feeds to the gasifier as another gasification agent. Thus, a mixture of moisture removed from the waste and air will be the gasification agent for the gasifier. The syngas out of the gasifier preheats

both the feeding air (through GAP heat exchanger) and the feeding steam (through SG heat exchanger). This study assumes that waste preheats to about 150°C from its initial temperature. A comprehensive gas cleaning system removes all harmful particles such as chlorine, sulfur, etc. to a level tolerable by the SOFC. Ref. [18] presented and deliberated the syngas compositions step-by-step through the gas cleaning system.

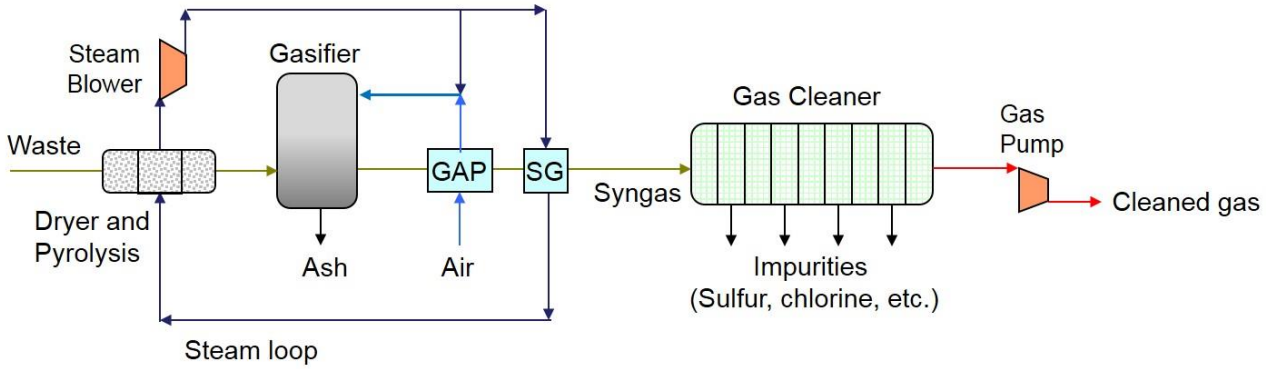

Figure 1: Gasifier plant with associated gas cleaning system modelled in this study. GAP = Gasifier Air Preheater, SG = Steam Generator.

As discussed above MW is a very heterogeneous resource and changes from country to country depending on lifestyle and income. Therefore, the present study assumes Denmark as the source for deciding the waste composition, see Table 1. Waste composition shown in Table 1 is based on the study of [19] through a comprehensive sampling and analysis for department stores.

Tabel 1: The compositions of the municipal waste used in this study [19], case of department stores.

Municipal Waste Composition	**Dry-based**
C (%)	45.39
H (%)	6.21
O (%)	26.56
N (%)	1.42
S + Cl (%)	0.16
Ash (%)	20.26
HHV (kJ/kg), (dry basis)	19990
c_p (kJ/kg)	1.84
Moisture (%)	18.12

2.3 Modeling of SOFC

The SOFC model adopted here aims on representing the performance of the second-generation planar SOFC developed the Fuel Cells and Solid State Chemistry Division at Risø–DTU (Technical University of Denmark) as explained in Ref. [20]. It is an anode-supported cell with a Ni/YSZ[1] anode, an YSZ electrolyte, and an LSM[2]/YSZ cathode as described in [21]. Anode thickness is 600 μm, electrolyte thickness is 50 μm and cathode thickness is 10 μm. The model showed an excellent agreement with the experimental data at different cell average operating temperatures, ranging from 650°C to 800°C (923K to 1073K). For sake of clarification, the model is briefly explained here. The model distinguishes between electro -chemical modeling, the calculation of cell irreversibility (cell

[1] Yttria-stabilized zirconia.
[2] Lanthanum strontium manganite.

voltage efficiency) and the calculation of the species compositions at the outlet. For the electrochemical modeling, the operational voltage (E_{cell}) is:

$$E_{cell} = E_{Nernst} - \Delta E_{act} - \Delta E_{ohm} - \Delta E_{conc} \quad (3)$$

where E_{Nernst}, ΔE_{act}, ΔE_{ohm} and ΔE_{conc} are the Nernst ideal reversible voltage, activation polarization, ohmic polarization and concentration polarization, respectively. The study assumes that hydrogen is the only electrochemical converting ions in the Nernst equation because electrochemical oxidation rate of H_2 is much higher than that of CO, (see e.g. [22]).

Butler–Volmer equation expresses the activation polarization by isolating this polarization from other polarizations and thereby determining the charge transfer coefficients and the exchange current density using experimental date available for different cell operating temperatures, the curve fitting technique (see, e.g. [23]).

The ohmic polarization depends on the electrical conductivity of the electrodes as well as the ionic conductivity of the electrolyte (see, e.g. [24]). This study calibrates the ohmic polarization against experimental data for different cell operating temperatures and for specified anode thickness, electrolyte thickness and cathode thickness as explained in Ref. [13].

The concentration polarization is dominant at very high current densities, wherein insufficient amounts of reactants transport to the electrodes resulting in blocking the pathway and consequently considerable decrease in cell voltage. Again, the current study uses experimental data to calibrate the concentration polarization for different cell operating temperatures by introducing the anode limiting current (see, e.g. [25]), and through inclusion of anode porosity, tortuosity and diffusion coefficient as explained in [13].

This study uses the Gibbs minimization method to calculate the fuel composition at the anode outlet, as described in [17] and through assumption of equilibrium at the anode outlet temperature and pressure for the species. Further, the Gibbs minimization method calculates the compositions of the species at the outlet by minimizing their Gibbs energies. The equilibrium assumption is fair because the methane content in this study is very low. Furthermore, the methane content is mainly depended on the kinetic parameters rather than the chemical equilibrium and its reaction rate is fast [26].

To calculate the voltage efficiency of the SOFC cells, the power production from the SOFC (P_{SOFC}) depends on the amount of chemical energy fed to the anode, the reversible efficiency (η_{rev}), the voltage efficiency (η_v) and the fuel utilization factor (U_F). Mathematically it can be expressed as

$$P_{SOFC}\left(LHV_{H_2}\dot{n}_{H_2,in} + LHV_{CO}\dot{n}_{CO,in} + LHV_{CH_4}\dot{n}_{CH_4,in}\right)\eta_{rev}\eta_v U_F \quad (4)$$

where U_F is a set value and η_v is defined as

$$\eta_{\mathrm{v}} = \frac{\Delta E_{\mathrm{cell}}}{E_{Nernst}} \quad (5)$$

The reversible efficiency is the maximum possible efficiency, defined as the relationship between the maximum electrical energy available (change in Gibbs free energy) and the fuel lower heating value (LHV) as discussed in e.g. [26].

In addition, Ref. [12] justified the reliability of the model/plant presented here with similar studies in the literature in terms of different fuels such natural gas, ethanol, and methanol. As an example, the calculated plant efficiencies by the current model agreed very well with the data presented in the literature for similar plant design.

Table 2 displays the main parameters for the SOFC stacks used in this study. These values are set for the basic case but can vary as discussed in [13], for example, this study assumes the value of

67.5% for the utilization factor. This study uses the mass flow in simple channel for assumption of pressure drops. Number of cell per stack and number of stacks are based on the previous studies [12], [13].

Table 2: The main SOFC parameters used in this study.

Parameter	Value
Fuel utilization factor	to be decided (0.7)
Number of cells in stack	75
Number of stacks	160
Cathode pressure drop ratio (bar)	0.04
Anode pressure drop ratio (bar)	0.01
Cathode inlet temperature (˚C)	600
Anode inlet temperature (˚C)	650
Outlet temperatures (˚C)	780

2.4 Modeling of Double Stage Lithium Bromide Absorption Chiller (AC) and its Validation

Absorption cycles are similar to vapor compression cycle, except instead of a vapor compressor (electricity driven) it uses a thermal compressor known as desorber or generator. Such thermal energy applies on a solution consisting of a refrigerant and an absorbent such as the mixture of water with lithium-bromide (LiBr) or, water with ammonia. Multiple-effect absorption cycle makes use of multiple generators (for example, two in double-stage cycle). The main reason for implementing multiple generators is to achieve improvements in the coefficient of performance (COP) by taking the advantage of higher availability of high temperature heat source [27]. This study uses the mixture of water with lithium-bromide in a double-stage chiller with one internal heat exchanger as indicated in Fig. 2.

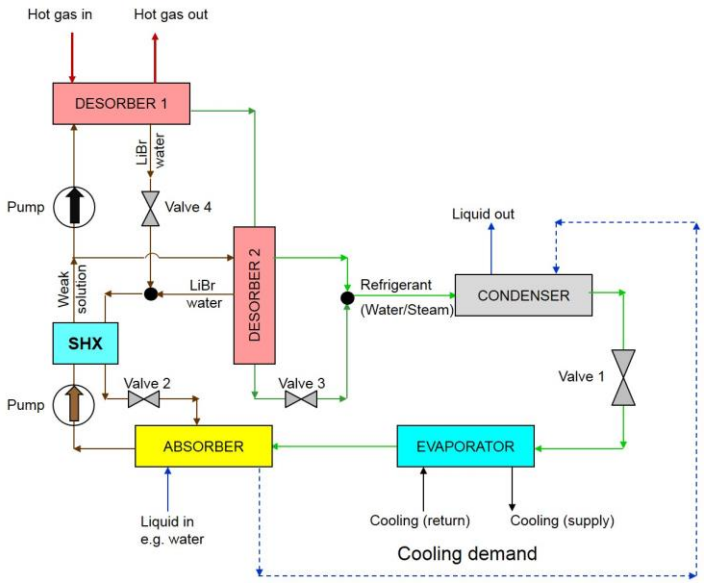

Figure 2: Double-stage absorption plant with internal solution heat exchanger (SHX).

The generator supply heat to the solution of LiBr-water and thereby separates some of the refrigerant from the solution mixture, creating a weak and rich solution. The amount of separation depends on the amount of heat supplied and the pressure of the mixture. The weak solution routes to a second generator, which then works as a heat supplement for a mixture with lower pressure. Thus, the second generator separates additional refrigerant from the mixture. The weak solution routes to a condenser to lose some heat and then to a valve to lose some pressure. Now the weak solution can

evaporate immediately if a proper amount of heat extracts from it. After evaporation. The weak solution, which has a very low pressure, routs to an absorber. The rich solution from the first generator enter a valve to lose some pressure and then mixes with the rich solution from the second generator. The mixed rich solution enter a solution heat exchanger to lose some heat and thereby heating up the original (diluted) solution. This rich solution is now enter the absorber. The absorber creates a low-pressure area that sucks the rich solution into the weak solution. The diluted solution out of the absorber is then pumped to the solution heat exchanger and the cycle repeats. Both the absorber and condenser reject heat to a cooling liquid such as water and therefore a cooling liquid enters to the absorber and then continuous to the condenser.

Note that in the present study, the heat input to the absorption chiller is the waste heat from the SOFC plant. This study assumes that the cooling flow enters the evaporator at 11°C and leaves it at 4°C. Table 3 shows the temperature of the cooling entering the absorber and leaving the condenser along with other parameters used in this study. Additionally, this study takes into account the properties of lithium-bromide solution mixture such as enthalpy, entropy and heat capacity from the open literature such as in [28].

Table 3: The main parameters for absorption chiller, basic case. SHX =Solution Heat Exchanger

Parameter	Value
Desorber gas outlet temperature (°C)	90 (basic case)
Rich solution (–)	0.6195
Week solution (–)	0.548
Condenser outlet temperature (°C)	32
Pressure after valve 1 (bar)	0.008
Pressure after valve 3 (bar)	0.05
Absorber cooling inlet temperature (˚C)	20
Absorber cooling inlet pressure (bar)	16
Hot side outlet temperature for SHX (˚C)	70
Solution pump pressure high/low (bar)	0.8/0.05

The present double stage AC provides a COP of about 1.17, which is much higher than the corresponding value for a single stage about 0.7, see e.g. [15]. The COP of AC is defined as

$$COP_{AC} = \frac{Q_{evaporator}}{Q_{desorber}} \tag{6}$$

where $Q_{evaporator}$ and $Q_{desorber}$ are the cooling demand and heat input to the desorber respectively.

Table 4 presents the model comparison with the study of [29]. As seen the model improved here under-predicts the COP compared with [29] by about 10%. However, if one applies two solution heat exchangers with the same data as in study of [30], then the model developed here gives a COP of 1.27 which is differs by about 3.8% with COP of [30] which is 1.32. Using the same data of the manufacture [31] with two solution heat exchangers then the present study gives a COP of 1.17, which is very close to the COP of manufacture [31] reported as 1.15.

Table 4: Comparison of the absorption chiller developed here with literature.

Reference / Parameter	YPC [29] 1 SHX*
Desorber inlet/outlet temperature (°C)	183.9 / 90
Cooling temperature supply/return (°C)	6.6 / 12.2
Absorber inlet temperature (°C)	29.4
Condenser outlet temperature (°C)	35
COP (–)	1.19

COP of the model developed here (–)	1.07
Deviation	10.08 %

* SHX = solution heat exchanger

2.5 Modeling of Direct Contact Membrane Distillation (DCMD) and its Validation

For this component, the present study uses a hollow fiber configuration, as described in [32]. Membrane distillation is a thermally driven membrane separation process, which involves the transport of water vapor through micro-porous hydrophobic membranes from aqueous solutions. The driving force for mass transfer in the process is vapor pressure difference across the membrane caused by temperature difference across the membrane. Among various membrane distillations, DCMD is the simplest mode since it does not require any external condenser when compared to vacuum membrane distillation and sweep gas membrane distillation. Membrane distillation can yield highly purified distillate, which operates under mild operating conditions, allowing to be applied in many applications such as desalination of seawater and brackish water, see e.g. [32] and [33]. The size of the pores are essential to allow only water vapor (without contamination) to pass through. One of the major disadvantages in the commercialization of membrane distillation is its relatively low permeate flux compared to other separation techniques, such as reverse osmosis. Therefore, designing a module with a very high packing density is extremely important.

Figure 3 shows the DCMD plant while Table 5 presents data related to the DCMD used here. The design of freshwater unit is rather simple. Seawater is preheated by freshwater and by a heat source (SwP1 and SwP2 heat exchangers in the figure, respectively) before entering the DCMD. In this study, the heat source is the off-heat provided by the fuel cell. Note that the freshwater loop is closed loop and is drives by a small water pump.

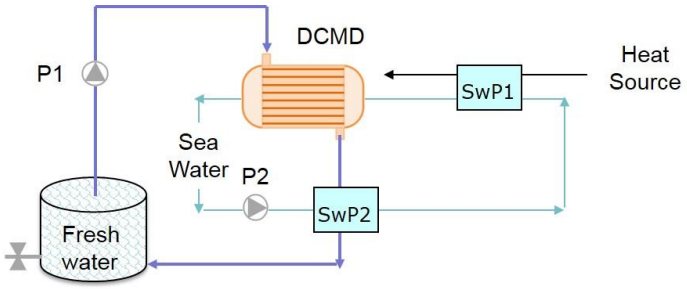

Figure 3: Scheme of a DCMD plant. Seawater preheats by freshwater (SwP2) and then by a heat source (SwP1).

Further, a tank collects the freshwater, while the non-desalinated seawater goes back into the sea again. The salt and other particles attached to the water molecules (larger sizes) cannot pass though the pores of the DCMD and therefore flows along the non-desalinated seawater to the sea. This study uses unit module parameters according to [33] such as fiber length, diameter, etc., shown in Table 5.

The range of operation of the model for one unit (module) is between 0.05–0.15 kg/s (according to the unit model used here). For larger mass flows, the model calculates the needed number of units. The range of operation for the feed temperature has limits, and in this study, it is set between 40°C to 90°C.

Another important issue to consider is the membrane liquid entry pressure, which sets the limit for the applied transmembrane pressure. Transmembrane pressure defines the difference between the hydrostatic pressure and the vapor pressure and therefore values below such limits will prevent liquid from entering the pores. The detailed mathematical model for this component is explained in [33].

To validate the model developed here the study of [34] and [35] are used. There are many different parameters to compare but one of the most relevant parameter is the transmembrane flux or water distilled depending on the inlet mass flow of the feed side. Assuming feed temperature to be 75°C and feed respective permeate mass flow to be 0.1 kg/s and 0.15 kg/s then the model gives 12 kg/m^{2}h

of freshwater, which is exactly the same as in [34]. Assuming permeate and feed temperatures of 25°C respective 70°C with feed flow of 0.49 kg/s (if density of water assumed being 850 kg/m^3 with 3.5% NaCl) then the model developed here gives 50 kg.m^{-2}.h^{-1} which is also the same as the study of [35].

Table 5: DCMD hollow fiber module specifications.

Parameter	Value
Fiber length	0.4 m
Inner diameter of fiber	0.3 mm
Membrane thickness	60 μm
Porosity	75%
Membrane conductivity	0.25 W/mK
Shell diameter	0.003 m
Number of fibers	3000
Packing density	60%
Inlet temperature	80°C
C_k (individual contribution of Knudsen diffusion)	15.18×10^{-4} [–]
C_m (individual contribution of Molecular diffusion)	5.1×103 m^{-1}
C_p (individual contribution of Poiseuille flow)	12.97×10^{-11} m

An important point regarding the DCMD plant is its efficiency. Since such plant produces freshwater in terms of [kg/s] then such dimension should change into effect [kW], which can be done by taking into account the efficiency of the DCMD plant. The efficiency of the DCMD plant is thus defined as

$$\eta_{DCMD} = \frac{\dot{m}_{FW,out}h_{FW,out} - \dot{m}_{FW,in}h_{FW,in}}{(\dot{m}_{SW,out}h_{SW,out} - \dot{m}_{SW,in}h_{SW,in}) + Q_{DCMD,in}} \quad (7)$$

where $\dot{m}$ and h are the mass flow and enthalpy. FW and SW refers to freshwater and seawater respectively. $Q_{DCMD,in}$ is the heat supplied to the DCMD units which is through the heat exchanger SwP1 shown in Fig. 3. Thus the term Q_{FW} is Eq, (1) shall be defined as

$$Q_{FW} = \eta_{DCMD} Q_{DCMD,in} \quad (8)$$

which means that parts of the energy supplied to the DCMD plant will change into freshwater, not all of it.

Another interesting parameter to be defined is the COP of DCMD which is defined as

$$COP_{DCMD} = \frac{\dot{m}_{freshwater}}{\dot{m}_{seawater}} \quad (9)$$

where $\dot{m}_{freshwater}$ and $\dot{m}_{seawater}$ are the mass flow of the freshwater from the DCMD and mass flow of the seawater to the DCMD respectively. The DCMD efficiency indicate how much of the energy feed into the unit is used to fresh up the seawater while its COP indicates how much of the seawater converts to the freshwater.

3. The Proposed Poly-generation System

Figure 4 represents the system proposed here. MW feeds a gasifier to produce syngas via a two-step process. The syngas temperature (after the gasifier plant) depends exclusively on the waste composition and its humidity. For the waste used in this study the syngas temperature is well over

200°C (473 K) and the partial pressure of steam is above 2, which enables simpler designing of the gas cleaning system than for the cold gas cleaning system.

Owing to stringent environmental regulations in many industrial countries, the syngas cleaning systems are getting simpler than the exhaust cleaning system after combustion [36]. For small size plants, silicon carbide filters and/or electromagnetic filters would likely be sufficient for syngas particle purification. However, if the plant size is increased, then the fuel conditioning system may also contain cyclones and/or scrubbers prior to silicon-based filters (or electromagnetic filters). Depending on the origin/type of waste then catalytic cleaning system may also be required to decrease the sulfur and chlorine level to the acceptable levels, 1 ppm respective 10 ppm. It is also worth noting that practical engineering may be more complicated than thermodynamic analyses. It is also assumed that by separating the gasifier into two steps then it would be possible to pyrolysis and gasify the waste that is well separated from metals, glasses, hard plastics, hard papers, etc. Such waste contains mainly waste foods, organics, some plastics, some papers, etc. Note that such cleaning system may take some of the energy and alter some results but this study does not consider such effect since the detailed cleaning system is missing.

For the SOFC plant shown in Fig. 4, includes a heat exchanger called for anode preheater (AP) which preheats the cleaned syngas (after the gasifier and the cleaning system) prior to the anode side of the fuel cell. Such preheating is essential to avoid fuel cell thermal fatigue, e.g. 130°C (403 K) for about 10–15 cm long cell, which has a thickness in μm. This study uses the off-fuel (unreacted fuel out of the anode side of the fuel cell) to preheat the fuel.

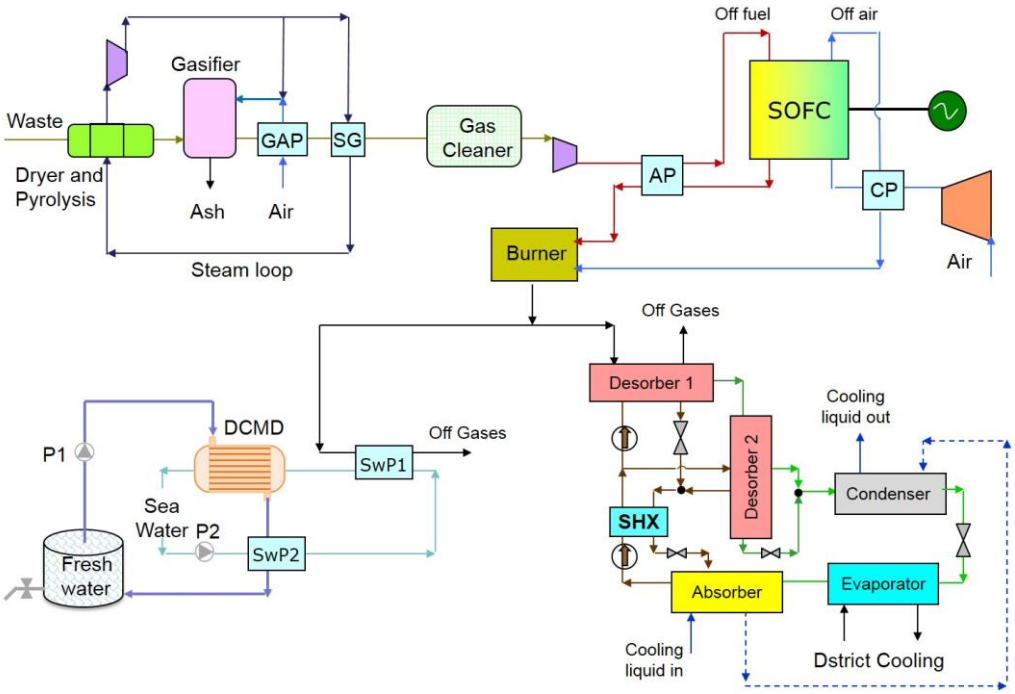

*Figure 4: Schematic of the suggested integrated waste gasification with SOFC, wherein seawater desalination and absorption chiller are **parallel** connected. AP = anode preheater, CP = cathode preheater, GAP = gasifier air preheater, SG = steam generator and SwP = seawater preheater.*

On the cathode side, air is first compressed and then preheated in a heat exchanger called for cathode preheater (CP) before entering the cathode side of the fuel cell. Such air preheating is vital to evade cell thermal tensions, e.g. 180°C for about 10–15 cm long and 10–20 μm thick cell. This study assumes the operating temperature of the fuel cell to be 780°C, and therefore this study uses the off-air, which is the unreacted air out of the cathode side, to preheat the incoming air. An after burner burns the unreacted fuel out of the anode side of the fuel cell utilizing the remaining oxygen from the cathode side of the fuel cell. The burner is required due to incomplete fuel utilization in the fuel cell.

As designed in Fig. 4, the waste heat after the SOFC plant then drives both DCMD and AC units simultaneously (parallel connection). The off-gasses after the burner are separated in a way that part of it goes to the DCMD unit and the rest goes to the AC unit. Thus, the amount of freshwater and productions can be controlled after demand. Note that the temperature after the burner is rather high, more than 420°C. Of course, this temperature also depends on the waste composition and its moisture content. For the base case, half of the off-gases drive the DCMD unit and the other half serves the AC unit.

The mass flow of the waste is assumed in a way that the system is able to produce electricity at about 120 kW suitable for decentralized location such as resorts, hotels, hospitals, shopping centers (Malls), etc. This study assumes a constant mass flow for the waste in order to have a fair comparison between the different proposed designs. Table 6 presents all other parameters assumed in this study.

Table 6: System operating input parameters.

Parameter	Value
MW mass flow (kg/h)	105.3
MW temperature (°C)	15
Drying temperature (°C)	150
Gasifier outlet temperature (°C)	800
Gasifier pressure (bar)	1
Gasifier pressure drop (bar)	0.005
Gasifier carbon conversion factor	1
Gasifier non-equilibrium methane	0.01
Steam blower isentropic efficiency	0.8
Steam blower mechanical efficiency	0.98
Air temperature into gasifier (°C)	15
Syngas blower isentropic efficiency	0.7
Syngas blower mechanical efficiency	0.95
Syngas cleaner pressure drop	0.0049
Blower air intake temperature (°C)	15
Blower isentropic efficiency	0.7
Blower mechanical efficiency	0.95
Gas heat exchangers pressure drop (bar)	0.01
Cathode preheater pressure drop (bar)	0.04
Anode preheater pressure drop (bar)	0.01
Burner inlet-outlet pressure ratio (efficiency)	0.95

Finally, it is also important to note that the realizability of such plant depends entirely on the technique of waste gasification and production of syngas suitable to feed the SOFC plant. Wärtsilä Corporation has already built two SOFC plants fueled by methanol and landfill gas, one as auxiliary unit in a ship and one as small power generator [37]. There are also some small SOFC units in the market for household applications. Further, The DCMD units has widely been evaluated experimentally, while the absorption chillers exist as commercial units in the market. Thus the realization of SOFC combined with AC should technically be possible, if one neglect the associated cost. However, the gasification of municipal waste (after basic recycling techniques) to produce a syngas suitable to feed SOFC is challenging and some technical problems must be solved, before integrating it with the combined SOFC–DCMD–AC plant.

4. Results and discussions

One important parameter to be decided is SOFC fuel utilization factor (U_F) which means how much of the fuel to be utilizes within the length of the cells. Depending on the waste type and its composition, one needs to optimize this parameter to achieve the highest performance. Figure 5

displays the study carried out here. As shown increasing the current density (as well as SOFC utilization factor), decreases cell voltage slightly until a certain point where the electrolyte concentration increases so high (exponentially) that additional oxygen ions cannot cross it and therefor cell voltage suddenly decreases significantly and reached to zero, see Fig. 5b. Consequently, further increase in current density (or utilization factor) decreases plant efficiency dramatically, compare Fig. 5a and Fig. 5b. Figure 5a shows also that the plant performance in terms of electrical efficiency (Eq. 2) and net power production maximizes at utilization factor of 70%. This is why in all calculations here utilization factor is set to 70%. Again, the optimum SOFC utilization factor depends on the type of the feed fuel (type of waste) and may vary slightly if the composition of the fuel changes.

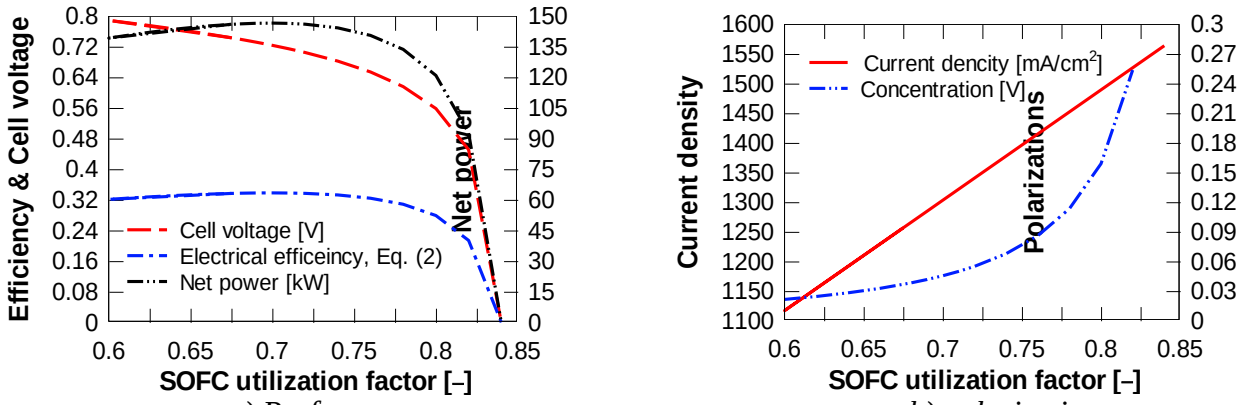

a) Performance *b) polarization*

Figure 5: Effect of SOFC utilization factor on a) plant performance, and b) polarization.

Table 7 presents the main results from the suggested plants. As established, the presented plant is able to produce about 146 kW of electricity with about 180 liter of freshwater per hour as well as about 145 kW of cooling effect simultaneously. The efficiency of the DCMD unit is about 59%, while the coefficient of performance (COP) of the AC unit is about 1.15 (cooling effect delivered by the evaporator to the heat input to the first desorber). Table 7 also reveals that the plant energy efficiency (including cooling and freshwater productions in addition to the electricity) is about 85%, which is well above the electrical (thermal) efficiency of the plant calculated as 34% (only electricity is the production). This in other words means that the waste heat has efficiently been used to produce other products (cooling and freshwater) besides electricity. As noted earlier, this study assumes the mass flow of waste to be 105.3 kg/hour.

Table 7: Plant performance.

Parameter	Values
Net electric production	146.56 kW
Freshwater production	179.94 kg/h
Heat input to DCMD, Q_{FW}	125.66 kW
DCMD efficiency	59.30 %
Cooling production	145.34 kW
Fuel consumption (LHV)	433.35 kW
Total power consumption	16.394 kW
Off-gases temp.	90°C (363 K)
Electric efficiency, Eq. (2)	33.82 %
Plant energy efficiency, Eq. (1)	84.55 %

4.1 Effect of Splitter Fraction between DCMD and AC for Parallel Connection

For the case with parallel DCMD and AC connection, one important parameter to be studied is the splitter fraction, which decides how much of the waste heat drives the DCMD units. Thus, in practice the splitter acts as a control valve. Here the splitter fraction is the fraction of the waste heat going to the DCMD units while the rest drives the AC unit. Figure 6 presents the results of such study. Increasing the splitter fraction (opening a valve to allow more mass flow goes through the AC unit) increases the cooling effect since more waste heat flows through the AC desorber. Figure 6a shows this effect. Thus, the cooling effect increases while freshwater production decreases which allows adjusting the production after demand. Opening the valve from 0% (closed) to 95% decreases freshwater production from 330 liter/hour to about 29 liter/hour (again, assuming water density is 1000 kg/m^3). At the same time cooling effect increases from zero to about 278 kJ/s. Opening the control valve decreases the inlet temperature for the seawater preheater (SwP2) at the hot side (less mass flow) and simultaneously increases the outlet temperature of the same heat exchanger. This means that the pinch temperature for this heat exchanger decreases steadily when the control valve opens. Thus, at a point, this pinch temperature will be very low and further opening of the control valve has no effect. This is the reason why Fig. 6 shows the values until splitter fraction is about 95%.

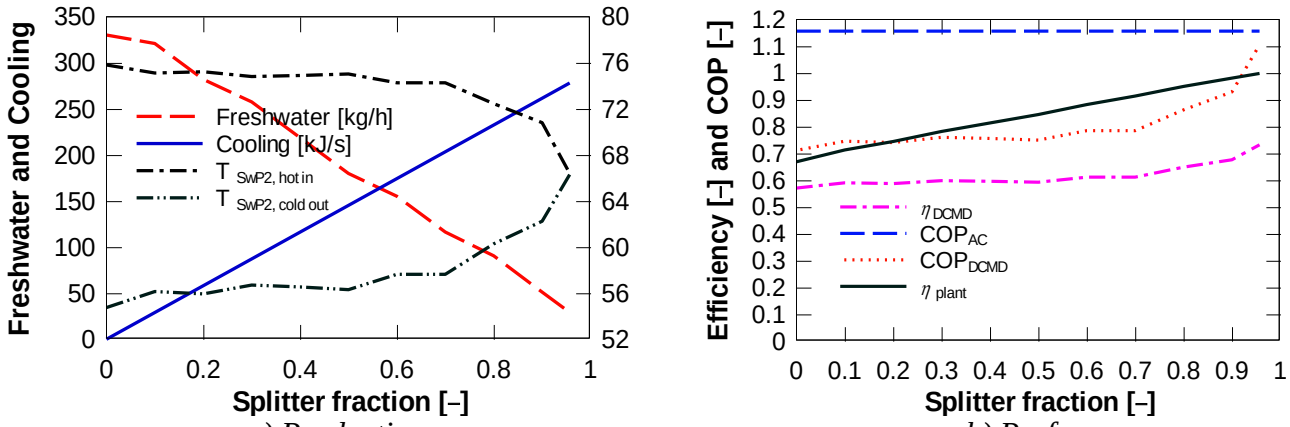

a) Production *b) Performance*

Figure 6: Plant performance as function of splitter fraction for parallel connection, a) freshwater and cooling production and b) performance.

Opening the valve (adjusting the demand) increases the performance of the DCMD unit (COP_{DCMD} which, is based on mass flows), see Fig. 6b. The reason is that more mass-flow goes through the DCMD unit and pinch temperature of the heat exchanger SwP2 decreases at the same time. The performance of AC remains unchanged (1.15) since the AC design does not change. However, the efficiency of the DCMD plant increases from 57% to 73% when the valve opens gradually (lower pinch temperature for SwP2). Consequently, plant total efficiency (energy efficiency) increases gradually (from 67% to more than 90%). In this case, the COP of the DCMD increases from 0.71 to 1.1, which is a significant improvement.

4.2 Effect of Waste Moisture Content

Moisture content may vary from day to day depending on the consumption and waste and therefore, this study looks into its effect on plant performance. Effect of moisture content on plant performance is another interesting point for studying. The higher the moisture content is, the lower net power production will be, as displayed in Fig. 7a. Increasing moisture content results in lower after burner temperature, which in turn means less heat, is available for bottoming cycles (AC and DCMD units). Figure 7b reveals such results. Consequently, productions of cooling and freshwater decreases also, as shown in Fig. 7a.

Higher moisture content means also that fuel energy decreases (c.f. HHV in Table 1) and this is why the plant electrical efficiency remains almost unchanged despite decreasing net power production, as displayed in Fig. 7b.

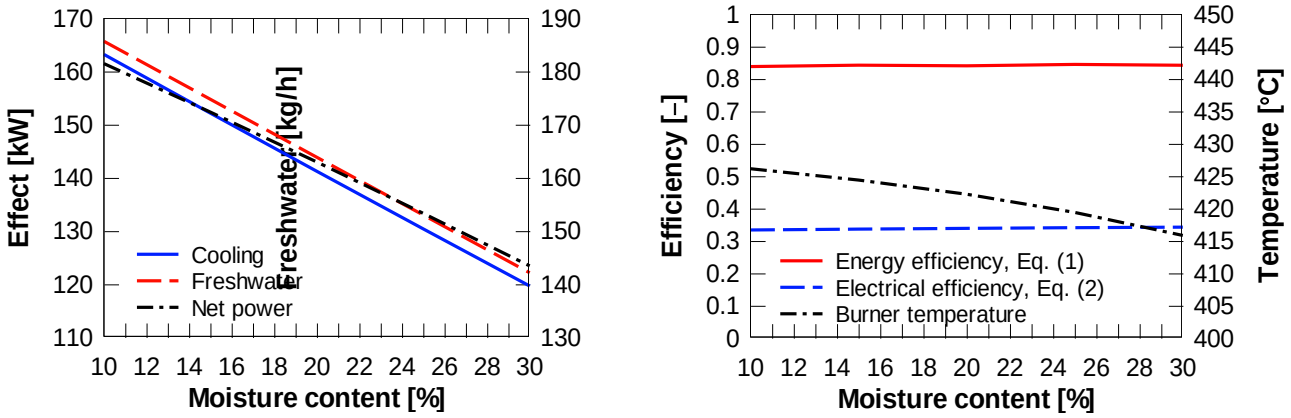

a) Effect *b) Performance*

Figure 7: Plant performance and effect as function of moisture content in the waste, a) effect and b) performance.

5. Conclusions

This study presented a thermodynamic analysis of a poly-generation system based on municipal waste, solid oxide fuel cell, seawater desalination and abruption chiller. Some results from this study may be:

- The electrical efficiency of the plant is about 34% with a net power of 145 kW.
- Connecting the absorption chiller and seawater desalination systems in *parallel* as bottoming cycle for the fuel cell plant then freshwater and cooling productions will be about 180 liter/hour and 145 kW respectively when waste heat from SOFC plant divides equally between AC and DCMD plants.
- The suggested designs offer the possibility to regulate freshwater and cooling productions after demand.
- Effect production (electricity, cooling and freshwater) depends on the moisture of the feed waste while plant total efficiencies (electrical and energy) does not change significantly.

References

[1] Lee, K.H. and Strand, R.K.: SOFC cogeneration system for building applications, part 2: System configuration and operating condition design. Renewable Energy, 34(12), pp. 2839–2846 (2009).

[2] Niessen, W.R.: Combustion and Incineration Processes: Applications in Environmental Engineering, fourth ed. CRC Press, Massachusetts, USA (2010).

[3] Buah, W.K., Cunliffe, A.M., Williams, P.T.: Characterization of products from the pyrolysis of municipal solid waste. IChemE, 85, pp. 450–457 (2007).

[4] Worldwide Gasification Database (GSTC), Waste to Energy Gasification, accessed October 2018. https://www.globalsyngas.org/syngas-production/waste-to-energy-gasification/.

[5] Arafat, H.A., Jijakli. K.: Modeling and comparative assessment of municipal solid waste gasification for energy production. Waste Management, 33, pp. 1704–1713 (2013).

[6] Couto, N.D., Silva, V.B., Rouboa, A.: Thermodynamic Evaluation of Portuguese municipal solid waste gasification. Journal of Cleaner Production, 139, pp. 622–635 (2016).

[7] Ionescu, G., Rada, E.C., Ragazzi, M., Marculescu. C,. Badea, A., Apostol, T.: Integrated municipal solid waste scenario model using advanced pretreatment and waste to energy processes. Energy Conversion and Management, 76, pp. 1083–1092 (2013).

[8] Bandara, N.J.G.J., Hettiaratchi, J.P.A., Wirasinghe S.C., Pilapiiya, S.: Relation of waste generation and composition to socio-economic factors: a case study. Environmental Monitoring and Assessment, 135, pp. 31–39 (2007).

[9] Caton, P.A., Carr, M.A., Kim, S.S., Beautyman, M.J.: Energy recovery from waste food by combustion or gasification with the potential for regenerative dehydration: A case study. Energy Conversion and Management, 51, pp. 1157–1169 (2010).

[10] Zhao, L., Wang, H., Qing, S., Liu, H.: Characteristics of gaseous product from municipal solid waste gasification with hot blast furnace slag. Journal of Natural Gas Chemistry, 19, pp. 403–408 (2010).

[11] Riensche, E., Achenbach, E., Froning, D., Haines, M.R., Heidug, W.K., Lokurlu, A., Adrian, S.: Clean combined-cycle SOFC power plant–cell modeling and process analysis. Power Sources, 86(1–2), pp. 404–410 (2000).

[12] Rokni ,M.: Thermodynamic Analysis of an Integrated Gasification Plant with Solid Oxide Fuel Cell and Steam Cycle. J GREEN, 2(2–3), pp. 71–86 (2012).

[13] Rokni, M. Thermodynamic analysis of SOFC (solid oxide fuel cell) – Stirling hybrid plants using alternative fuels. Energy, 61, pp. 87–97 (2013).

[14] Tippawan, P., Arpornwichanop, A., Dincer, I.: Energy and exergy analysis of an ethanol-fueled solid oxide fuel cell for a trigeneration system. Energy, 87, pp. 228–239 (2015).

[15] Joneydi Shariatzadeh, O., Refahi, A.H., Rahmani, M., Abolhassani, S.S.: Economic optimisation and thermodynamic modelling of SOFC tri-generation system fed by biogas. Energy Conversion and Management, 105, pp. 772–781 (2015).

[16] Elmegaard, B., Houbak, N.: DNA - A general energy system simulation tool. Proceeding of SIMS 2005, Trondheim, Norway. Eds: Amundsen J, Andersson HI, Celledoni E, Gravdahl T, Michelsen FA, Nagel HR and Natvig T. Oct 13 – 14, 2005. ISBN: 9781617388729. Pages 43 – 52.

[17] Smith, J.M., Van Ness, H.C., Abbott, M.M.: Introduction to chemical engineering thermodynamics. 7th edition, Boston: McGraw-Hill (2005).

[18] Rokni, M.: Thermodynamic analyses of municipal solid waste gasification plant integrated with solid oxide fuel cell and Stirling hybrid system. Hydrogen Energy, 40, pp. 7855–7869 (2015).

[19] Edjabou, M.E., Jensen, M.B., Götze, R., Pivnenko, K., Petersen, C., Scheutz, C., Fruergaard Astrup, T.. Municipal solid waste composition: Sampling methodology, statistical analyses, and case study evaluation. Waste Management, 36, pp. 12–23 (2015).

[20] Petersen, T.F., Houbak, N., Elmegaard, B.: A zero-dimensional model of a 2nd generation planar SOFC with calibrated parameters. Int. J. Thermodynamic, 9(4), pp. 161–169 (2006).

[21] Christiansen, N., Primdahl, S., Wandel, M., Ramousse, S., Hagen, A.: Status of the solid oxide fuel cell development at Topsoe Fuel Cell A/S and DTU Energy Conversion. J Electrochemical Society, 57(1), pp. 43–52 (2013).

[22] Holtappels, P., DeHaart, L.G.J., Stimming, U., Vinke, I.C., Mogensen, M.: Reaction of CO/CO2 gas mixtures on Ni-YSZ cermet electrode. Applied Electrochemistry, 29, pp. 561–568 (1999).

[23] Prentice, G.: Electrochemical Engineering Principles. Prentice Hall International, Houston, USA (1991).

[24] Zhu, H., Kee, R.J.: A general mathematical model for analyzing the performance of fuel-cell membrane-electrode assemblies. Power Sources, 117, pp. 61–74 (2003).

[25] Costamagna, P., Selimovic, A., Del Borghi, M., Agnew, G.: Electrochemical model of the integrated planar solid oxide fuel cell (IP-SOFC), Chemical Engineering, 102(1), pp. 61–69 (2004).

[26] Kromp, A., Leonide, A., Timmermann, H., Weber, A, Ivers-Tiffée, E.: Internal Reforming Kinetics in SOFC-Anodes. ECS Transactions, 28(11), pp. 205–215 (2010).

[27] Misra, R.D., Sahoo, P.K., Gupta, A.: Thermoeconomic optimization of a LiBr/H2O absorption chiller using structural method. Energy Resources Technology, 127, pp. 119–124 (2005).

[28] Patek, J., Klomfar, J.A.: Computationally effective formulation of the thermodynamic properties of LiBr-H2O solutions from 273 to 500 K over full composition range. Int. J. of Refrigeration, 29(4), pp. 566–78 (2006).

[29] Jhonson Controls.: Model YPC 2-Stage Steam-Fired Absorption Chiller Style D. Tech. rep. Form:155.19-EG3 (1011), Printed in USA, Milwaukee. [accessed: 29-08-2018], pp. 1–24 (2011), http://www.johnsoncontrols.com/~/media/jci/be/united-states/hvac-equipment/chillers/files/be_ypc_res_engineering-guide.pdf?la=en.

[30] Herold, K.E., Radermacher, R., Klein, S.A.: Absorption Chillers and Heat Pumps. CRC Press, (1996). ISBN: 0-8493-9427-9.

[31] Tozer, R. James, R.: Absorption chillers applied to CHP systems. Building Services Engineering Research and Technology, 16(4), pp. 179–188 (1995). ISSN: 14770849, 01436244. doi:10.1177/014362449501600.

[32] Cath, T.Y., Adams, V.D., Childress, A.E.: Experimental study of desalination using direct contact membrane distillation: a new approach to flux enhancement. Membrane Science, 228, pp. 5–16 (2004).

[33] Kim, Y.D., Thu, K., Ghaffour, N., Ng, K.C.: Performance investigation of a solar-assisted direct contact membrane. Membrane Science, 427, pp. 345–364 (2013).

[34] Cheng, L.H., Wu, P.C., Chen, J.: Modeling and optimization of hollow fiber DCMD module for desalination. Journal of Membrane Science, 318, pp. 154–166 (2008).

[35] Yang, X., Wang, R., Shia, L., Fane, A.G., Debowski, M.: Performance improvement of PVDF hollow fiber-based membrane distillation process. Journal of Membrane Science, 369, pp. 437–447 (2011).

[36] Morris, M., Waldheim, L.: Energy recovery from solid waste fuels using advanced gasification technology. Waste Management, 18(6-8), pp. 557–564 (1998).

[37] Babicz, J.: Wärtsilä Encyclopedia of Ship Technology. 2nd ed. Wärsilä Corporation, Helsinki (2015), ISBN: 978-952-93-5536-5.